$Fe(TPP)F$.[28] Column 5 in Table IV shows the hole sizes are essentially the same in $Fe(TPP)(OReO_3)$ and the high-spin acetate system. But we can note that the average Fe–N distances increase from 1.961 Å for $Fe(TPP)B_{11}CH_{12}$ to 2.059 Å for $Fe(TPP)(OReO_3)$ to 2.072 Å for $Fe(TPP)F$. Also, in the cases where there are Fe–O bonds, the distances decrease in a monotonic fashion from 2.067 Å in $Fe(OEP)(OClO_3)$ to 2.024 Å in $Fe(TPP)(OReO_3)$ to 1.898 Å in $Fe(TTP)OAc$.

These data place the amount of the $S = {}^3/_2$ state in the 20 ± 10% range in the admixture of $S = {}^3/_2$ and $S = {}^5/_2$ spin states for $Fe(TPP)(OReO_3)$·tol, which is the smallest amount thus far reported for Fe(TPP)X intermediate-spin systems.

Acknowledgment. We thank Richard Austin at the University of Texas in Austin for measuring the NMR spectra and Mrs. Cynthia Day of Crystalytics Co., Lincoln, NE, for collecting the X-ray data. B.B.H. (Grant No. B-483) and G.L.P. (Grant No. R-1054) thank The Robert A. Welch Foundation for their support of this work. G.J.L. thanks the donors of the Petroleum Research Fund, administered by the American Chemical Society, for support of this research.

Registry No. $Fe(TPP)(OReO_3)$, 95978-32-8; $Fe(TPP)(OReO_3)$·tol, 129916-89-8; $Fe(TPP)Cl$, 16456-81-8; $AgReO_4$, 7784-00-1.

Supplementary Material Available: Textual and tabular details of the crystal structure analysis and listings of bond distances, bond angles, anisotropic thermal parameters, and least-squares planes (14 pages); a table of observed and calculated structure factors (22 pages). Ordering information is given on any current masthead page.

---

(28) Anzai, K.; Hatano, K.; Young, J. L.; Scheidt, W. R. *Inorg. Chem.* **1981**, *20*, 2337.

Contribution from the Departments of Chemistry, Faculty of Science, Alexandria University, Alexandria, Egypt, and Northeastern University, Boston, Massachusetts 02115

Synthesis and Properties of Mixed-Valence Copper Molecules $(\mu\text{-}Y)N_4Cu^{II}_2Cu^{I}_2X_4$ (N = *N*,*N*-Diethylnicotinamide; Y = 3,4,5,6-Tetrachlorocatecholate; X = Cl, Br, I) and the Products and Kinetics of Their Reactions with Dioxygen in Nitrobenzene

Mohamed A. El-Sayed*[,1a] and Geoffrey Davies*[,1b]

Received December 18, 1989

Tetranuclear copper(I) complexes $[NCuX]_4$ (N = *N*,*N*-diethylnicotinamide; X = Cl, Br, I (Ia–c, respectively)) react stoichiometrically with equimolar 3,4,5,6-tetrachloro-1,2-benzoquinone (Cl_4BQ) under dinitrogen at room temperature in methylene chloride or nitrobenzene to give tetranuclear mixed-valence copper products $(\mu\text{-}Y)N_4Cu^{II}_2Cu^{I}_2X_4$ (Va–c, respectively), where Y is 3,4,5,6-tetrachlorocatecholate. The electronic spectra of Va–c contain maxima in the region 750–820 nm that are due to their copper(II) centers. The maximum molar absorptivities decrease as X is changed from Cl to Br to I and the corresponding wavelengths decrease when X is changed from Br to Cl to I. Molecules Va–c are oxidized by dioxygen in ambient nitrobenzene with stoichiometry $\Delta[VI]/[O_2] = 2.0 \pm 0.1$ to give tetranuclear mono(oxo)mono(catecholato)copper(II) complexes $(\mu\text{-}O,\mu\text{-}Y)[NCuX]_4$ (VIa–c, respectively). Products VI have larger maximum molar absorptivities than the respective products V in the 600–900-nm region. Absorptivity of VI is larger with X = Br than with X = Cl and smaller with X = I. The spectra of $(\mu\text{-}Y)_2[NCuX]_4$ (Y = O (II), CO_3, or 3,4,5,6-tetrachlorocatecholate (IV)) with fixed X = Cl or Br are very similar. Rhombic EPR spectra with four hyperfine lines for solid mixed-valence complexes Va–c at 300 K indicate trigonal-pyramidal geometry for their copper(II) centers with no evidence for significant copper(I)–copper(II) interactions. The EPR spectra of VIa–c in methylene chloride are isotropic at 300 K and rhombic with more than four hyperfine lines at 130 K, indicating more than one kind of copper(II) site. Comparison of the solid-state EPR spectra of $(\mu\text{-}O)_2[NCuCl]_4$ (IIa), IVa, Va, and VIa at 300K indicates that (a) IIa contains square-pyramidal copper(II), (b) solid IVa has different copper(II) centers despite having only one kind of bridge, and (c) the distinct copper(II) centers of VIa can be observed in the solid state. Cyclic voltammograms of Va and VIa–c at a Pt electrode in ambient methylene chloride are quasi-reversible (E^f = 0.51, 0.52, 0.61, and 0.59 V vs SCE, respectively). Complex Va is oxidized by O_2 to VIa with a third-order rate law, as found for the oxidation of copper(I) dimers $[LCuX]_2$, where L is an *N*,*N*,*N'*,*N'*-tetraalkyl diamine. Comparison of the kinetic data indicates assembly of an activated complex containing one O_2 and two Va molecules as the rate-determining step. By contrast, the corresponding oxidations of Vb and Vc are second-order processes, like those of complexes $[NCuX]_4$, $N_3Cu_3M(NS)X_4$, and $N_3Cu_3M(NS)_2X_4$ (NS = monoanionic *S*-methyl isopropylidenehydrazinecarbodithioate). The slowest steps appear to involve electron transfer from Vb and Vc to O_2. Respective intermediates IXb and IXc are rapidly reduced by excess Vb or Vc to the corresponding oxocopper(II) products VIb and VIc.

Introduction

There is a great deal of current interest in the structural,[2,3] chemical,[3-7] and photophysical properties of polynuclear halo(amine)copper(I) complexes because they are easily constructed, phosphorescent[8,9] polymetallic systems containing a common, catalytically active metal.[2,3,5] This paper further demonstrates their usefulness for generating mixed-valence copper complexes.[10]

Our work is concerned with the products and kinetics of the aprotic oxidation of polynuclear copper(I) complexes by dioxygen (for example, eq 1),[4] their transmetalation with $M(NS)_n$ reagents

$$\underset{\text{I}}{[NCuX]_4} + O_2 \rightarrow \underset{\text{II}}{(\mu\text{-}O)_2[NCuX]_4} \qquad (1)$$

$$I + M(NS)_2 \rightarrow N_3Cu_3M(NS)X_4 + N + Cu(NS)(s) \qquad (2)$$

$$N_3Cu_3M(NS)X_4 + O_2 + H_2O \rightarrow \underset{\text{III}}{(\mu_4\text{-}O,\mu\text{-}O)N_3Cu_3M(H_2O)X_4} + {}^1\!/_2N_2S_2 \qquad (3)$$

(eq 2)[7,10] and the reactions of the transmetalated derivatives with dioxygen (eq 3).[7,10] Here, N is a monodentate pyridine ligand,

---

(1) (a) Alexandria University; (b) Northeastern University.

(2) Caulton, K. G.; Davies, G.; Holt, E. M. *Polyhedron Rep.*, in press.

(3) Davies, G.; El-Sayed, M. A. In *Copper Coordination Chemistry: Biochemical and Inorganic Perspectives*; Karlin, K. D., Zubieta, J., Eds.; Adenine Press: Guilderland, NY, 1983; p 281 and references therein.

(4) Davies, G.; El-Sayed, M. A. *Inorg. Chem.* **1983**, *22*, 1257.

(5) Karlin, K. D.; Gultneh, Y. *Prog. Inorg. Chem.* **1987**, *35*, 219.

(6) (a) Churchill, M. R.; Davies, G.; El-Sayed, M. A.; Fournier, J. A.; Hutchinson, J. P.; Zubieta, J. A. *Inorg. Chem.* **1984**, *23*, 783. (b) El-Sayed, M. A.; El-Toukhy, A.; Davies, G. *Inorg. Chem.* **1985**, *24*, 3387.

(7) Davies, G.; El-Sayed, M. A.; El-Toukhy, A.; Gilbert, T. R.; Nabih, K. *Inorg. Chem.* **1986**, *25*, 1929.

(8) Vogler, A.; Kunkely, H. *J. Am. Chem. Soc.* **1986**, *108*, 7211. Hardt, H. D.; Pierre, A. *Inorg. Chim. Acta* **1977**, *25*, L59. Hardt, H. D.; Pierre, A. Z. *Anorg. Allg. Chem.* **1973**, *407*, 107. De Ahna, H. D.; Hardt, H. D. *Z. Anorg. Allg. Chem.* **1972**, *387*, 61.

(9) Henary, M.; Zink, J. I. *J. Am. Chem. Soc.* **1989**, *111*, 7407.

(10) (a) Davies, G.; El-Sayed, M. A.; El-Toukhy, A.; Henary, M.; Gilbert, T. R. *Inorg. Chem.* **1986**, *25*, 2373. (b) Davies, G.; El-Sayed, M. A.; El-Toukhy, A.; Henary, M.; Kasem, T. S.; Martin, C. A. *Inorg. Chem.* **1986**, *25*, 3904.

0020-1669/90/1329-4891$02.50/0

Table I. Analytical and Cryoscopic Data for Products Va–c and VIa–c

label	complex[b]	anal., %[a] C	H	N	X	Cu	M_r[c]
Va	$(\mu\text{-Y})[N_4Cu^{II}{}_2Cu^{I}{}_2Cl_4]$	39.8 (40.8)	4.2 (4.1)	8.0 (8.3)	21.3 (21.0)	18.7 (18.8)	1400 ± 30 (1355)
Vb	$(\mu\text{-Y})[N_4Cu^{II}{}_2Cu^{I}{}_2Br_4]$	36.5 (36.0)	3.4 (3.7)	7.4 (7.3)		17.0 (16.6)	1500 ± 30 (1535)
Vc	$(\mu\text{-Y})[N_4Cu^{II}{}_2Cu^{I}{}_2I_4]$	31.2 (32.1)	3.0 (3.3)	6.9 (6.5)		15.1 (14.8)	1700 ± 30 (1735)
VIa	$(\mu\text{-O},\mu\text{-Y})[NCuCl]_4$	39.6 (40.3)	4.2 (4.1)	7.9 (8.2)	18.0 (18.5)	17.6 (18.5)	1400 ± 30 (1370)
VIb	$(\mu\text{-O},\mu\text{-Y})[NCuBr]_4$	36.3 (35.7)	4.0 (3.6)	7.2 (7.2)		16.4 (16.4)	1600 ± 30 (1550)
VIc	$(\mu\text{-O},\mu\text{-Y})[NCuI]_4$	31.0 (31.8)	3.0 (3.2)	6.2 (6.5)		15.2 (14.6)	1800 ± 30 (1750)

[a] Calculated values in parentheses. [b] Y is 3,4,5,6-tetrachlorocatecholate. [c] Measured in nitrobenzene at the (3–5) × 10^{-2} *m* level.[4]

X is Cl or Br, M is Co, Ni, Cu, or Zn, NS is monoanionic *S*-methyl isopropylidenehydrazinecarbodithioate and N_2S_2 is the corresponding disulfide. The kinetic work is aimed at determining the mechanisms of important copper-catalyzed reactions of dioxygen.[3,5,11]

Reactions 1 and 3 result in the complete reduction of dioxygen to coordinated oxide in II and III because $[NCuX]_4$ and $N_3CuM(NS)X_4$ are four-electron reducing agents.[3,4,7,10–13] The proposed rate-determining step is insertion of O_2 through the halide cores of the respective reductants.[3,4,7,10–13]

Tetranuclear complexes $[NCuX]_4$ (N is *N,N*-diethylnicotinamide; X is Cl, Br, and I in Ia–c, respectively) react with 2 mol of 3,4,5,6-tetrahalo-1,2-benzoquinones Cl_4BQ and Br_4BQ according to eqs 4 and 5, where Y is the corresponding 3,4,5,6-

$$\text{Ia–c} + 2Cl_4BQ \rightarrow \underset{\text{IVa–c}}{(\mu\text{-Y})_2[N_4CuX]_4} \tag{4}$$

$$\text{Ia–c} + 2Br_4BQ \rightarrow (\mu\text{-Y})_2[N_4CuX]_4 \tag{5}$$

tetrahalocatecholate when X is Cl or Br and the corresponding semiquinone when X = I.[14] These reactions result from attack of the quinone oxidants on opposite faces of cubanes Ia–c and do not require penetration of their halide cores.[14]

The products of eqs 4 and 5 are interesting for two important reasons. First, they are electrochemically active, whereas copper(II) complexes $(\mu\text{-Y})_2[NCuX]_4$ (Y = O (II) or CO_3) are not.[3,4,14] Second, like $(\mu\text{-}(O,CO_3))_2[NCuX]_4$ complexes,[13,15] they can be transmetalated in stoichiometric steps with $M(NS)_2$ reagents to give isolated products $(\mu\text{-Y})N_4Cu_{4-x}M_xX_4(OH)_2{\cdot}3H_2O$ that also are electrochemically active.[14]

This paper reports that oxidant Cl_4BQ can be used to generate mixed valence molecules $(\mu\text{-Y})N_4Cu^{II}{}_2Cu^{I}{}_2X_4$ (Va–c) via eq 6,

$$\text{Ia–c} + Cl_4BQ \rightarrow \underset{\text{Va–c}}{(\mu\text{-Y})N_4Cu^{II}{}_2Cu^{I}{}_2X_4} \tag{6}$$

$$2\text{Va–c} + O_2 \rightarrow \underset{\text{VIa–c}}{2(\mu\text{-O},\mu\text{-Y})[NCuX]_4} \tag{7}$$

where Y is 3,4,5,6-tetrachlorocatecholate and X = Cl, Br, and I, respectively. Also reported are the products and kinetics of aprotic oxidations of excess Va–c with dioxygen, which give tetranuclear copper(II) complexes $(\mu\text{-O},\mu\text{-Y})[NCuX]_4$ (VIa–c), reactions 7. The rate laws of reactions 7 depend on X in V. The properties of Va–c and VIa–c are described, and the kinetics of reactions 7 are compared with those for aprotic oxidations of other polynuclear halo(amine)copper(I) complexes by dioxygen.

Experimental Section

Materials. Nitrobenzene was distilled under reduced pressure from P_2O_5 and stored over 4-Å molecular sieves. Methylene chloride was purified as described previously.[4] High-purity dinitrogen was deoxygenated by passage through a column of Alfa DE-OX solid catalyst. Copper(I) halides CuX were prepared as described in the literature.[16] *N,N*-Diethylnicotinamide (N, Aldrich) was distilled under reduced pressure immediately before use. Oxidant 3,4,5,6-tetrachloro-1,2-benzoquinone (Cl_4BQ, Aldrich) and tetrabutylammonium perchlorate (Eastman polarographic grade) for electrochemical measurements were used as received.

Synthesis of Mixed-Valence Molecules Va–c. Solid CuX (10.0 mmol) was added to a deoxygenated solution of N (10.0 mmol) in methylene chloride (30 mL) and the mixture was stirred at room temperature under dinitrogen until a clear solution (for X = Cl or Br) or a milky suspension (for X = I) of $[NCuX]_4$ (Ia–c) was obtained.[4] Brown solutions of the respective complexes Va–c resulted from addition, under dinitrogen, of 2.50 mmol of Cl_4BQ either as a solid or as a deoxygenated solution in methylene chloride (25 mL). The solution was then stirred under dinitrogen for 1 h to ensure completion of reaction 6. Solid samples of Va–c were obtained by vacuum solvent evaporation at room temperature and stored under dinitrogen. Attempts to grow single crystals of Va–c were unsuccessful. Analytical and cryoscopic molecular weight data are given in Table I.

Synthesis of Mono(oxo)mono(catecholato)copper(II) Molecules VIa–c. Depending on X (see kinetic data below), dry dioxygen was bubbled for 30 min to 2 h through a solution of the respective complexes V in methylene chloride at room temperature. Brown solid products VIa–c were obtained by vacuum solvent evaporation at room temperature. Attempts to grow single crystals of VIa–c were unsuccessful. Analytical and cryoscopic molecular weight data are given in Table I.

Physical Measurements. The electronic spectra of Va–c and VIa–c in methylene chloride or nitrobenzene (Table II) were measured under dinitrogen with Beckman DK-1A and DB-G spectrophotometers in matched quartz cells at room temperature. EPR spectra of solids Va–c and VIa–c or 1.0 mM solutions of these complexes in methylene chloride were recorded at 100 kHz and 6.28 G modulation amplitude in methylene chloride were recorded at 100 kHz and 6.28 G modulation amplitude on a Bruker Electrospin Model ESP 300 spectrometer. Incident power was 100 mW. Resonance conditions were found at ca. 9.39 GHz (X-band) at room temperature and 130 K. Cyclic voltammograms were recorded with a Bioanalytical Systems CV-1B instrument connected to a Honeywell Model 530 X-Y recorder. A platinum working electrode (Beckman) and a platinum-wire auxilliary electrode were employed in all measurments. Samples of Va and VI were dissolved in deoxygenated methylene chloride containing 0.1 M tetrabutylammonium perchlorate as the supporting electrolyte. All solutions were kept under dinitrogen during electrochemical measurements. All potentials were measured with respect to a saturated calomel electrode (SCE) and referenced to the potential of the ferrocenium/ferrocene couple (0.40 V).[17]

The stoichiometry of reactions 7 was determined from dioxygen uptake data with a standard Warburg apparatus at room temperature.[4] Kinetic measurements of reactions 7 were made by monitoring absorbance increases as a function of time at fixed wavelength in the region 750–850 nm. Oxidation of Va was monitored with a Hi-Tech Scientific Model SFL41 stopped-flow spectrophotometer with Va in pseudo-first-

---

(11) El-Sayed, M. A.; Abu-Raqabah, A.; Davies, G.; El-Toukhy, A. *Inorg. Chem.* **1989**, *28*, 1909.

(12) Davies, G.; El-Sayed, M. A. *Comments Inorg. Chem.* **1985**, *4*, 151.

(13) Davies, G.; El-Sayed, M. A.; El-Toukhy, A. *Comments Inorg. Chem.* 1989, *8*, 203.

(14) El-Sayed, M. A.; El-Toukhy, A.; Ismael, K. Z.; El-Maradne, A. A. *Inorg. Chim. Acta*, in press.

(15) (a) El-Toukhy, A.; Cai, G.-Z.; Davies, G.; Gilbert, T. R.; Onan, K. D.; Veidis, M. *J. Am. Chem. Soc.* **1984**, *106*, 4596. (b) Cai, G.-Z.; Davies, G.; El-Toukhy, A.; Gilbert, T. R.; Henary, M. *Inorg. Chem.* **1985**, *24*, 1701.

(16) Keller, R. N.; Wycoff, H. D. *Inorg. Synth.* **1946**, *2*, 1.

(17) Gritzer, G. *Inorg. Chim. Acta* **1977**, *24*, 5. Gagne, R. R.; Koval, C. A.; Lisensky, G. C. *Inorg. Chem.* **1980**, *19*, 2854.

Table II. EPR and Electronic Spectral Data for Complexes V and VI

			EPR					
complex	state	temp[a]	g_1	g_2	g_3	$\langle g \rangle$	g_i	λ_{max}, nm (ϵ_λ, M^{-1} cm^{-1})[b]
Va	*c*	*d*	2.46	2.08	2.01	2.18		850 (440), 775 (470)
Vb	*c*	*d*	2.47	2.07	2.02	2.19		825 (320), 750 (300)
Vc	*c*	*d*	2.47	2.09	1.98	2.18		825 (93), 740 (110)
VIa	*b*	*d*					2.13	850 (785), 765 (750)
	b	*e*	2.51	2.08	2.03	2.21		
VIb	*b*	*d*					2.13	850 (1140), 775 (1070)
	b	*e*	2.51	2.07	2.02	2.20		
VIc	*b*	*d*					2.14	825 (155), 765 (165)
	b	*e*	2.53	2.08	2.06	2.22		

[a] Temperature in K. [b] In methylene chloride (1.0 mM). [c] Solid state. [d] Temperature is 300 K. [e] Temperature is 130 K.

order excess. The oxidations of Vb and Vc were monitored by conventional techniques with a Perkin-Elmer Lambda 4 spectrophotometer. Kinetic orders and rate constants for the oxidations of Vb and Vc were determined by initial rate measurements ($[\mathrm{Vb,c}]_0/[\mathrm{O}_2]_0 = 0.50{-}2.50$) and the activation parameters were established with Vb,c in excess. The total reactant concentration range was $[\mathrm{V}]_0 = (8.3{-}45.0) \times 10^{-4}$ M, with $[\mathrm{O}_2]_0 = (4.4{-}14.7) \times 10^{-4}$ M. Temperature was controlled to ±0.05 °C in the range 10.0–48.0 °C. Pseudo-first-order rate constants k_{obsd} were obtained from the slopes of linear plots of log ($A_\infty - A_t$) vs time, where A_t is the absorbance at fixed wavelength and temperature at the time t. Each run was repeated at least three times under fixed experimental conditions to establish an upper limit of ±5% for each reported rate constant.

Results and Discussion

General Observations. Benzoquinones $\mathrm{Cl_4BQ}$ and $\mathrm{Br_4BQ}$ readily oxidize the air-stable copper(I) complex $[\mathrm{NCuI}]_4$ (Ic) in reactions 4 and 5.[14] They can also be used to make mixed-valence products Va–c in stoichiometric reactions 6 under dinitrogen. Another simple chemical way of making mixed-valence derivatives of cubanes Ia,b is by anaerobic transmetalation (eqs 8; M is Co[10] or Fe[18]). Transmetalation accompanied by electron transfer from

$$\mathrm{Ia,b} + \mathrm{M(NS)_3} \rightarrow \underset{\mathrm{VIIa,b}}{\mathrm{N_3Cu^I{}_2Cu^{II}M(NS)_2X_4}} + \mathrm{N} + \mathrm{Cu(NS)(s)} \tag{8}$$

$$\mathrm{VIIa,b} + \mathrm{O_2} \rightarrow \underset{\mathrm{IIIa,b}}{(\mu_4\text{-O},\mu\text{-O})\mathrm{N_3Cu_3MX_4}} + \mathrm{N_2S_2} \tag{9}$$

$$\mathrm{d[III]/d}t = k_\mathrm{T}[\mathrm{VII}][\mathrm{O_2}] \tag{10}$$

copper(I) to M(III) results in absorption bands in the 500–900 nm region that are due to copper(II) and M(II) in mixed-valence products VIIa,b.[10,18] Molecules $\mathrm{N_3Cu_3M(NS)X_4}$ (eq 2) and VIIa,b are rapidly oxidized by dioxygen (compare eqs 3 and 9).[7,10] The second-order rate law, eq 10, is characteristic of the oxidation of tetranuclear halo(amine)copper complexes that contain at least three copper(I) centers (see below).[3,4,7,10] The core structures of dioxotetrametal products IIIa,b can be distinguished from other structural alternatives (for example, II (Chart I)) by a number of techniques.[7,10,18-20]

Spectra and Proposed Core Structure of Mixed-Valence Molecules Va–c. The analytical and cryoscopic data in Table I identify products Va–c from eqs 6 as discrete tetranuclear molecules. Their infrared spectra in KBr disks or methylene chloride contain a single band at 1640 cm^{-1} that indicates monodentate N bonded through its pyridine nitrogen atom.[22]

The electronic spectra of Va–c (Table II and Figure 1) are typical of tetranuclear oxo(halo)(pyridine)copper(II) complexes whose copper(II) centers are bonded to three halide ligands.[22] The maximum molar absorptivities decrease as X is changed from Cl to Br to I. This ordering is different in the corresponding oxo(catecholato)copper(II) products VIa–c from eqs 7 (see below). We propose the core structure in Chart I for complexes V.[23,24]

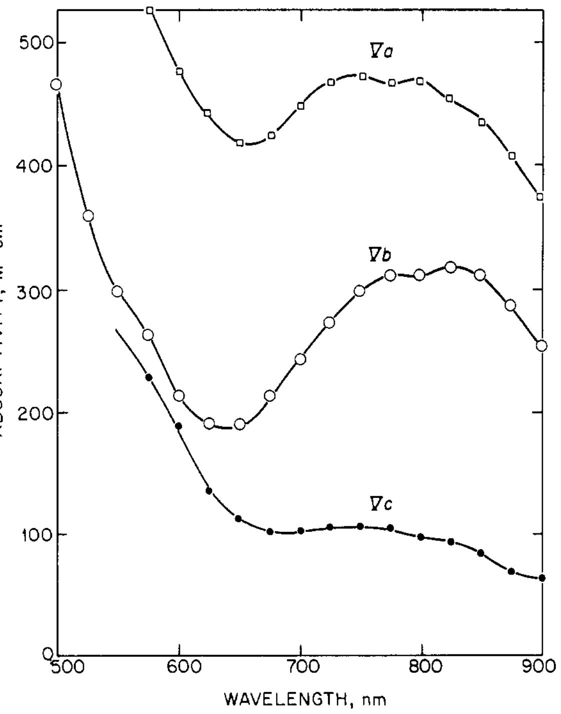

Figure 1. Electronic spectra of Va–c in nitrobenzene at 25 °C.

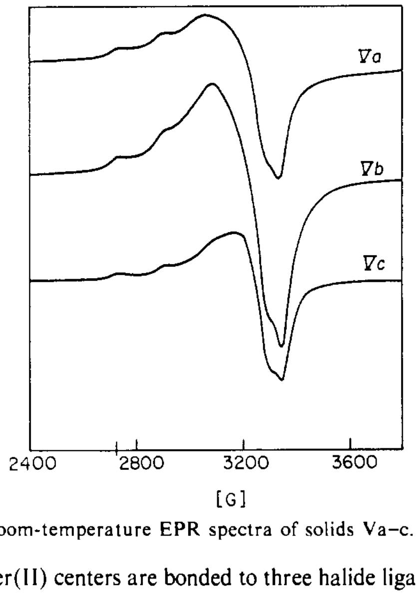

Figure 2. Room-temperature EPR spectra of solids Va–c.

---

(18) Davies, G.; El-Sayed, M. A.; El-Toukhy, A.; Henary, M. *Inorg. Chim. Acta* **1990**, *168*, 65.

(19) Tetranuclear complexes $[\mathrm{NCuX}]_4\mathrm{Y}_2$ (Y = O, $\mathrm{CO_3}$, or 3,4,5,6-tetrachlorocatecholate) characteristically disproportionate on attempted crystallization,[4,14,20,21] which necessitates the use of a variety of techniques (including transmetalation patterns)[13,14] to distinguish between their alternative core structures.[20,21]

(20) Davies, G.; El-Sayed, M. A.; El-Toukhy, A.; Henary, M.; Martin, C. A. *Inorg. Chem.* **1986**, *25*, 4479.

(21) Henary, M.; Davies, G.; Abu-Raqabah, A.; El-Sayed, M. A.; El-Toukhy, A. *Inorg. Chem.* **1988**, *27*, 1872.

(22) Davies, G.; El-Toukhy, A.; Onan, K. D.; Veidis, M. *Inorg. Chim. Acta* **1985**, *98*, 85.

(23) Attempted crystallization of products Va–c and VIa–c by a variety of techniques results in disproportionation to unidentified products.[19]

Chart I

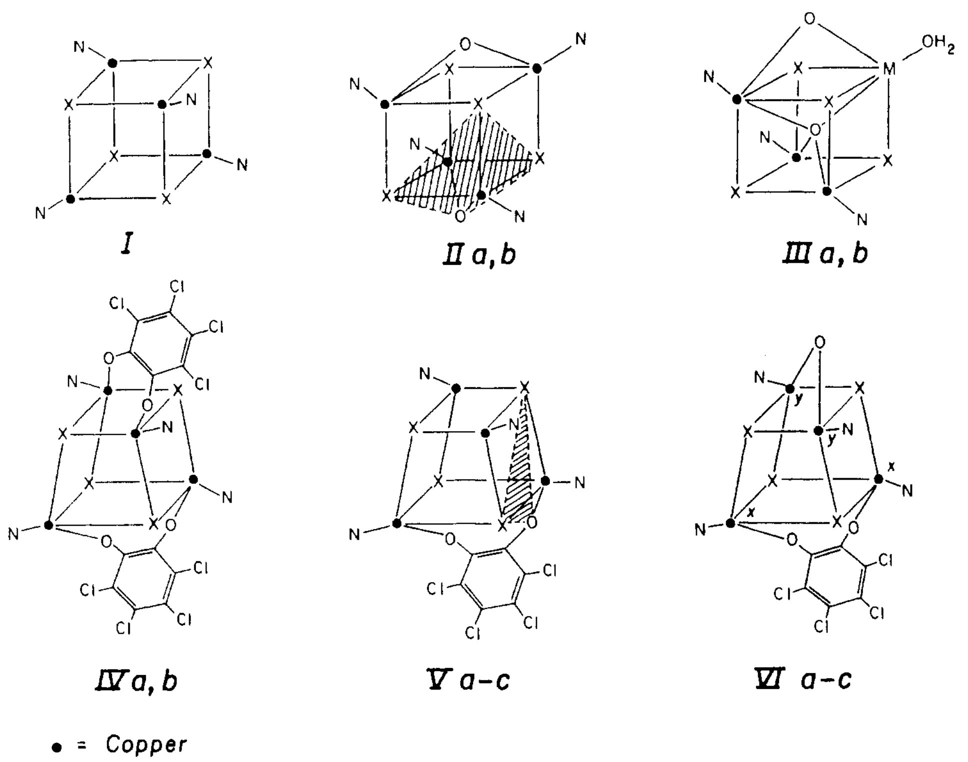

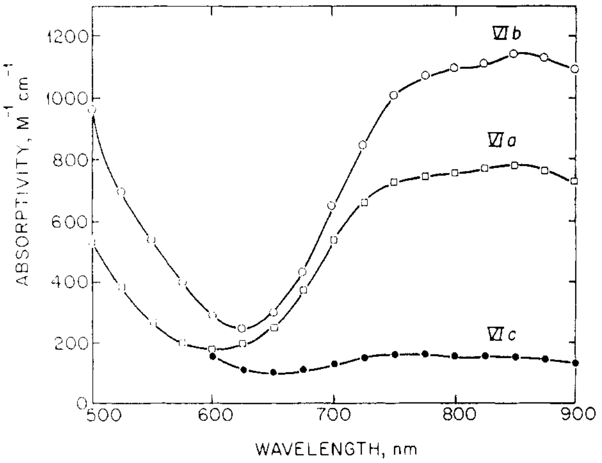

Figure 3. Electronic spectra of VIa-c in nitrobenzene at 25 °C.

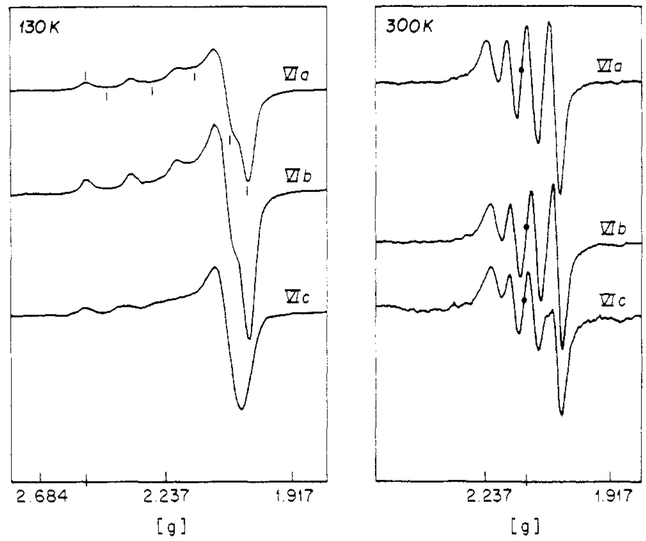

Figure 4. EPR spectra of complexes VIa-c (1.0 mM) in methylene chloride.

Room-Temperature Solid-State EPR Spectra of Va-c. The room-temperature solid-state EPR spectra of Va-c under dinitrogen are shown in Figure 2 and summarized in Table II. These complexes display classical rhombic spectra that indicate trigonal-pyramidal geometry about one type of (catecholato)copper(II) site.[25] The detection of only four hyperfine lines indicates little, if any, interaction between the copper(I) and copper(II) centers of V.

Stoichiometry of Reactions 7. Dioxygen uptake measurements by standard Warburg manometry showed that reactions 7 proceed with stoichiometry $\Delta[\mathrm{VIa{-}c}]/\Delta[\mathrm{O_2}] = 2.0 \pm 0.1$ in nitrobenzene at 25 °C. This information and the electronic spectra in Figures 1, 3, and 4 indicate that the two copper(I) centers of Va-c are oxidized but that their bridging catecholate ligands are not oxidized. The analytical and cryoscopic data in Table I identify the oxidation produducts as discrete tetranuclear mono(oxo)mono(catecholato)copper(II) molecules (μ-O,μ-Y)[NCuX]$_4$ (VIa-c).

Spectra and Proposed Core Structure of Products VIa-c. The infrared spectra of products VIa-c in KBr disks or methylene chloride solution contain a single band at 1640 cm^{-1} that indicates monodentate N bonded through its pyridine nitrogen atom.[22] The electronic spectra of VIa-c (Figure 3 and Table II) are typical of tetranuclear oxo(halo)(pyridine)copper(II) complexes in which each copper(II) center is bonded to three halide ligands.[22]

Increases of absorptivity occur in the 700-950 nm region when Va-c are oxidized to VIa-c in reactions 7 (compare Figures 1 and 3). The increase is approximately 2-fold when X = Cl or I, indicating that the distinct copper(II) sites *x* and *y* in products VIa and VIc (Chart I) have about the same atomic absorptivity. By contrast, the maximum molar absorptivities of Vb and VIb differ by a factor of ca. 3.5 at 850 nm (compare Figures 1 and 3). This indicates that the atomic absorptivity of the copper(II) at sites *y* in VIb is larger than that at sites *x* (Chart I).

---

(24) There is considerable current interest in the spectral and other properties of mixed valence systems; see, for example: reference 9. Lippard, S. J., Ed. *Progress in Inorganic Chemistry*; Wiley: New York, 1983; Vol. 30. Zhang, L.-T.; Ko, J.; Ondrechen, M. J. *J. Phys. Chem.* **1989**, *93*, 3030.

(25) Hathaway, B. J. In *Comprehensive Coordination Chemistry*; Wilkinson, G., Gillard, R. D., McCleverty, J. A., Eds.; Pergamon: Oxford, England, 1985; Vol. 5, p 534.

The electronic spectra of $(\mu\text{-Y})_2[NCuX]_4$ molecules (Y = O (IIa,b),[4] CO_3,[26] or 3,4,5,6-tetrachlorocatecholate (IVa,b)[14]) are closely similar to those of the respective products VIa,b. Molar absorptivities are generally larger with X = Br, as also observed here (Figure 3). This similarity leads to the proposed core structure in Chart I for complexes VI.[23]

The oxidative stability of tetranuclear iodo(pyridine)copper(I) complexes enables their easy synthesis and crystallization.[2,26] It is due to (a) their characteristic insolubility in solvents like methylene chloride and nitrobenzene, (b) greater stabilization of copper(I) by iodide than by chloride and bromide, and (c) presumed greater difficulty of insertion of O_2 through the I_4 cores of $[NCuI]_4$ molecules than in the rate-determining step for oxidation of the corresponding chloro and bromo analogues.[4,7,10] Reactions 4, 5, and 7 provide the only reported access to discrete iodo(pyridine)copper(II) molecules. We note that iodocopper complexes Vc and VIc have much less intense spectra than their chloro and bromo analogues.

No Reaction with CO_2. Reaction 11 is characteristic of $(\mu\text{-O})_2[NCuX]_4$ molecules II (X = Cl or Br) and their transmetalated derivatives.[3,4,15,20,26,27] However, prolonged exposure of VIa–c to CO_2 at 1 atm resulted in no reaction either in the solid state or in methylene chloride.

$$\text{II} + 2CO_2 \rightarrow (\mu\text{-}CO_3)_2[NCuX]_4 \qquad (11)$$

This lack of reactivity toward CO_2 resembles that observed for products IIIa,b of reactions 3 and 9.[7,10] The explanation offered[7,10] for this behavior was that tight copper(II) binding by the central μ_4-oxo group in IIIa,b results in very acute Cu-O-M angles in the μ-oxo bridges of these molecules (Chart I): $(\mu\text{-O})_2[NCuX]_4$ molecules II contain no such central group and their Cu–O–Cu angles evidently can open to accommodate the linear Cu–O–Cu arrangements in known (μ-carbonato)copper(II) complexes.[28] Our proposed core structure for VI (Chart I) contains a very acute Cu–O–Cu unit that evidently cannot react with CO_2 to give a μ-CO_3-bridged carbonato derivative.[29]

EPR Spectra of VIa–c. The room-temperature EPR spectra of VIa–c (1.0 mM) in methylene chloride at 300 and 130 K are shown in Figure 4 and summarized in Table II. Isotopic spectra with $g_i = 2.13$ are observed at 300 K. Cooling to 130 K results in rhombic spectra with more than four hyperfine lines. This indicates that molecules VI contain more than one distinct copper(II) site.[25]

Comparison of the Room-Temperature Solid-State EPR Spectra of $(\mu\text{-O})_2[NCuCl]_4$ (IIa), $(\mu\text{-Y})_2[NCuCl]_4$ (IVa), $(\mu\text{-Y})[NCuCl]_4$ (Va), and $(\mu\text{-O},\mu\text{-Y})[NCuCl]_4$ (VIa). In Figure 5, we compare the room-temperature solid-state EPR spectra of the title complexes. Our objective is to demonstrate that complexes IVa and VIa contain distinct copper(II) sites.

Dioxocopper(II) complex IIa displays a classical axial spectrum ($g_\parallel = 2.28$ ($A_\parallel = 133 \times 10^{-4}$ cm^{-1}); $g_\perp = 2.03$) that is diagnostic of a square-pyramidal geometry for copper(II).[25] This four-line spectrum indicates the presence of just one type of copper(II) site in IIa. As noted earlier, the mixed-valence molecule Va displays a rhombic spectrum (Table II) with four hyperfine lines. A rhombic spectrum is expected for trigonal-bipyramidal geometry about copper(II).[25] There is no ESR evidence for significant copper(I)–copper(II) interactions in V.

By contrast, the spectrum of solid $(\mu\text{-O},\mu\text{-Y})[NCuCl]_4$ (VIa) contains more than four hyperfine lines, which is to be expected because complexes VI contain distinct sites *x* and *y* (Chart I).

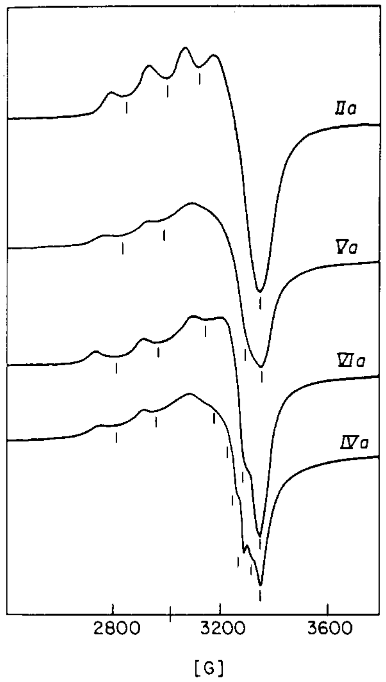

Figure 5. Room-temperature EPR spectra of solid complexes $(\mu\text{-O})_2[NCuCl]_4$ (IIa), $(\mu\text{-Y})[NCuCl]_4$ (Va), $(\mu\text{-O},\mu\text{-Y})[NCuCl]_4$ (VIa) and $(\mu\text{-Y})_2[NCuCl]_4$ (IVa).

The spectrum of solid $(\mu\text{-Y})_2[NCuCl]_4$ (IVa)[14] (Figure 5) also contains more than four hyperfine lines, despite the fact that it contains only one kind of bridge. It appears that the Cu···Cu separations in the catecholate-bridged faces of IVa are different and that this gives rise to distinct copper(II)–catecholate sites in these molecules. The bridging catecholate in the face with the shorter Cu···Cu separation is lost (as YH_2) in reaction 12, as also observed for transmetalated derivatives $(\mu\text{-Y})_2N_4Cu_{4-x}Ni_xCl_4$ of IVa.[14]

$$\text{IVa} + 5H_2O \rightarrow \underset{\text{VIIIa}}{N_4Cu_4(OH)_2Cl_4Y\cdot 3H_2O} + YH_2 \qquad (12)$$

Electrochemical Properties of Va and VIa–c. The cyclic voltammetric behavior of complexes Va and VIa–c (0.3–2.1 mM in methylene chloride) was examined. The supporting electrolyte was tetrabutylammonium perchlorate (0.1 M). For comparison, we also examined the electrochemical properties of Y^{2-} obtained by adding a 5-fold excess of pyridine to YH_2 in the same electrolyte solution. Typical data are shown in Figure 6.

Voltammograms are quasi-reversible in the scan range 50–200 mV s^{-1}, as indicated by i_{pa}/i_{pc} ratios greater than unity, where i_{pa} and i_{pc} are the peak anodic and cathodic currents in the scan range 50–200 mV s^{-1}. The greatest deviation from unity was i_{pa}/i_{pc} = 3.0–3.6 for VIa. The derived formal potentials E^f of Y^{2-}, Va, and VIa–c are 0.42, 0.51, 0.52, 0.61, and 0.59 V vs SCE, respectively. The maximum error in these measurements is ±20 mV.

These observations indicate that the copper–catecholate units in Va and VIa–c are electrochemically active and that coordination to copper(II) has only a moderate effect on E^f when X = Cl. However, E^f is significantly larger when X is Br or I in VIb or VIc, respectively.

Kinetics of Reactions 7. We now come to another interesting discovery: the rate laws for oxidation reactions 7 differ with X in reactants V.

Kinetics of Oxidation of Va by Dioxygen. The reaction of excess Va with dioxygen in nitrobenzene to give VIa (eq 7 (X = Cl), Table I) is governed by the irreversible third-order rate law 13. Typical results are shown in Figure 7 and the kinetic data are collected in Table III.

$$d[\text{VIa}]/dt = k_D[\text{Va}]^2[O_2] \qquad (13)$$

Comparison and Interpretation of Kinetic Data. Two-electron reductants $[LCuX]_2$ (L is an *N,N,N′,N′*-tetraalkyl diamine; X

---

[26] Churchill, M. R.; Davies, G.; El-Sayed, M. A.; Hutchinson, J. P.; Rupich, M. W. *Inorg. Chem.* **1982**, *21*, 995.

[27] Churchill, M. R.; Davies, G.; El-Sayed, M. A.; Hutchinson, J. P. *Inorg. Chem.* **1982**, *21*, 1002.

[28] Churchill, M. R.; Davies, G.; El-Sayed, M. A.; El-Shazly, M. F.; Hutchinson, J. P.; Rupich, M. W. *Inorg. Chem.* **1980**, *19*, 201.

[29] Complexes $(py)_3Cu_4X_4O_2$ and $(py)_4Cu_4X_4O_2$ (py = pyridine) also do not form carbonato derivatives, in this case because they contain μ_4-oxo and terminal oxo groups.[4,20]

[30] Addison, A. W.; Rao, T. N.; Sinn, E. *Inorg. Chem.* **1984**, *23*, 1957.

[31] Patterson, G. S.; Holm, R. H. *Bioinorg. Chem.* **1975**, *4*, 257.

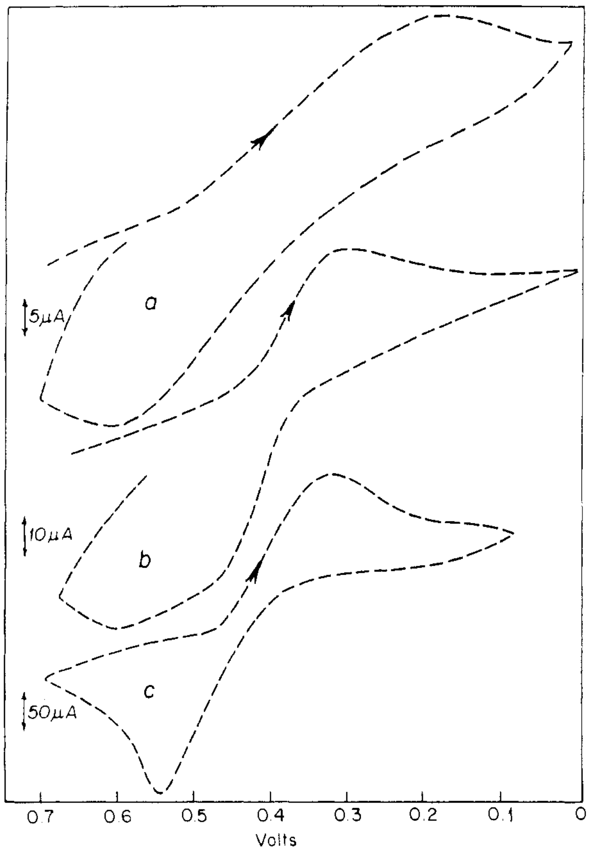

Figure 6. Cyclic voltammetric data for VIa (a), VIb (b), and VIc (c) in methylene chloride containing 0.1 M tetrabutylammonium perchlorate at 25 °C. The scan rate ν is 200 mV s^{-1} in all cases.

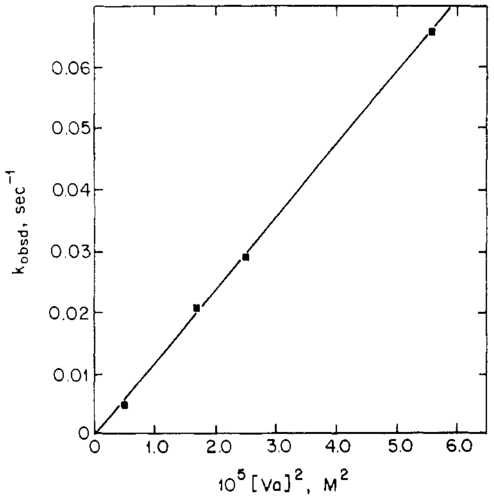

Figure 7. Plot of k_{obsd} vs $[Va]^2$ for the oxidation of Va by dioxygen in nitrobenzene at 19.0 °C.

is Cl or Br) are oxidized by dioxygen in aprotic solvents to the corresponding dimeric (μ-oxo)copper(II) complexes $[LCuX]_2O$ at ambient temperatures.[6] The reactions have a third-order rate law, as found for oxidation of Va (eq 13). The third-order rate constants k_D at 25 °C in nitrobenzene vary from 0.55 × 10^3 to 1360 × 10^3 M^{-2} s^{-1}, depending on L and X.[6b] k_D values are lower (by factors of 1–24) in methylene chloride and are always lower when X is changed from Cl to Br with fixed L. This information and data collected at low temperatures[32] indicate that assembly of an activated complex containing one O_2 and two $[LCuX]_2$ molecules is the rate-determining step.[6b,32]

The third-order rate constant k_D for oxidation of Va Table III is at the lower limit of the range of measured rate constants for oxidation of $[LCuX]_2$ dimers at ambient temperatures.[6b] A linear plot of $\Delta H_D^\ddagger$ vs $-\Delta S_D^\ddagger$ accommodates the data from Table III of ref 6b within experimental error. The $\Delta H_D^\ddagger$ value for oxidation of Va is about 2 kcal mol^{-1} greater than expected from the other data (Figure S1).[33] Tetranuclear mixed-valence molecule Va thus behaves as a halo(amine)copper(I) dimer in its aprotic reaction with dioxygen. Assembly of an activated complex containing one O_2 and two Va molecules seems to be the rate-determining step in the oxidation of Va to VIa.

Table III. Kinetic Data for the Oxidation of Va–c by Dioxygen in Nitrobenzene

(a) Third-Order Oxidation of Va

temp, °C	$10^{-3}k_{13}$,[a] M^{-2} s^{-1}	$\Delta H_{13}^\ddagger$,[b] kcal mol^{-1}	$\Delta S_{13}^\ddagger$,[c] cal deg^{-1} mol^{-1}
10.0	9.1		
19.0	12.6		
26.0	20.9		
41.0	39.9	8.7	−14

(b) Second-Order Oxidation of Vb,c

reductant	temp, °C	10^3k_{14},[d] M^{-1} s^{-1}	$\Delta H_{14}^\ddagger$,[b] kcal mol^{-1}	$\Delta S_{14}^\ddagger$,[c] cal deg mol^{-1}
Vb	11.0	160		
	20.0	200		
	30.0	280		
	41.5	430	6.6	−21
Vc	18.0	4.8		
	27.0	6.7		
	34.0	11.0		
	48.0	18.0	9.2	−38

[a] Rate law 13. [b] Typical error is ±0.4 kcal mol^{-1}. [c] At 25 °C. Typical error is ±5 cal deg^{-1} mol^{-1}. [d] Rate law 14.

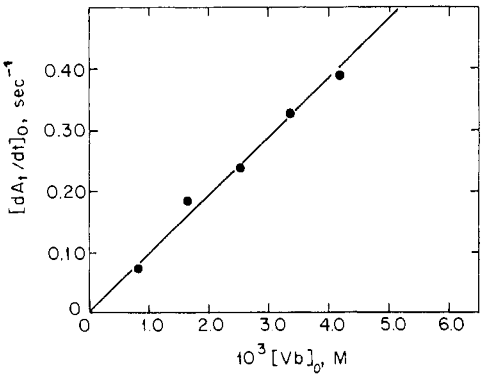

Figure 8. Plot of initial rate vs $[Vb]_0$ for the oxidation of Vb by dioxygen in nitrobenzene at 22.5 °C. $[O_2]_0$ is 7.33 × 10^{-4} M.

Kinetics of Oxidation of Vb and Vc by Dioxygen. In sharp contrast with the results of the previous section, the aprotic oxidations of Vb,c to their respective products VIb,c (Table I) by dioxygen are governed by the irreversible second-order rate law 14. Typical results are shown in Figure 8 and the kinetic data are collected in Table III.

$$\text{rate} = k_{14}[\text{Vb or Vc}][O_2] \qquad (14)$$

Comparison and Interpretation of Kinetic Data. Since reactions 1,[4] 3,[7] and 9[10a] and the oxidations of Vb,c by dioxygen are all second-order processes (eqs 10 and 14, respectively), it is appropriate to compare rate constants k_T and k_{14} and their associated activation parameters.

Reactions 1, 3, and 9 are governed by the second-order rate law 10 with rate constants k_T.[4,7,10a] When X is Cl, they characteristically have $\Delta H_T^\ddagger$ = 2–6 kcal mol^{-1} and very negative $\Delta S_T^\ddagger$ = −(38–49) cal deg^{-1} mol^{-1}. Changing X to Br results in decreased rates because $\Delta H_T^\ddagger$ increases by 2–5 kcal mol^{-1} with the same order of magnitude for $\Delta S_T^\ddagger$. These and other data indicate

---

(32) Davies, G.; El-Sayed, M. A.; Henary, M. *Inorg. Chem.* **1987**, *26*, 3266.

(33) Supplementary material.

Scheme I

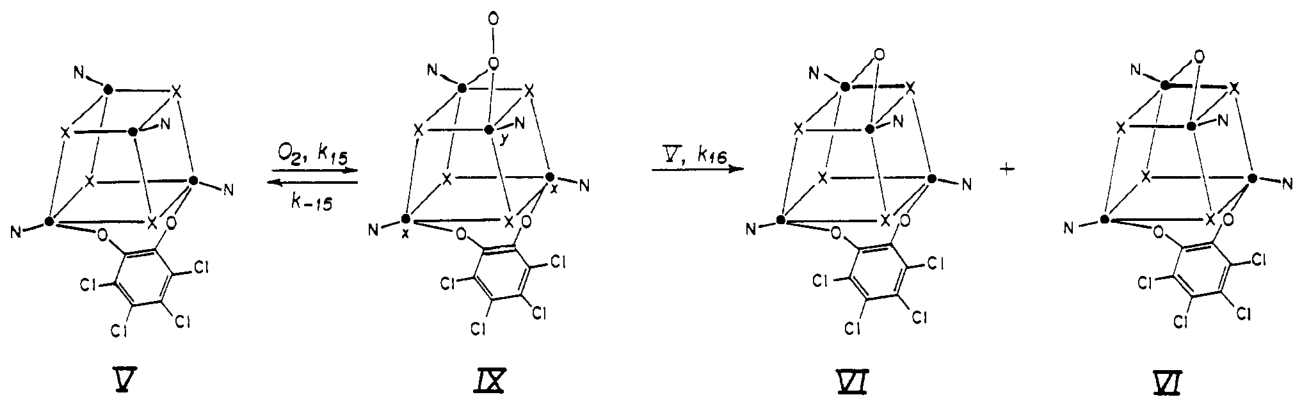

dioxygen insertion into the halide cores of the reductants as the rate-determining step.[3,4,7,10-13]

When X = Br, $10^3 k_T$ for reactions 1, 3, and 9 varies from 26 to 990 M^{-1} s^{-1} at 25 °C in nitrobenzene.[34] Rate constant k_{14} for oxidation of Vb is intermediate in this range, but that for Vc is lower (by a factor of ca. 5, Table III). The proposed core structure of Va-c (Chart I) contains bridging catecholate on one face that would seriously impede O_2 insertion through that face. Since products VIa-c are *mono*(μ-oxo)copper(II) complexes, insertion of O_2 through the halide cores of Va-c is unnecessary for their formation.[35]

It is much more likely that the oxidations of V proceed as shown in Scheme I. Assumption of a steady-state concentration for the respective intermediates IX gives eqs 15 and 16.

$$[IX] = k_{15}[V][O_2]/(k_{-15} + k_{16}[V]) \qquad (15)$$

$$d[VI]/dt = 2k_{16}[V][IX] = 2k_{15}k_{16}[V]^2[O_2]/(k_{-15} + k_{16}[V]) \qquad (16)$$

Equation 16 has two obvious limits. The first, $k_{-15} \gg k_{16}[V]$, gives eq 17. The second, $k_{-15} \ll k_{16}[V]$, gives eq 18.

$$d[VI]/dt = 2K_{15}k_{16}[V]^2[O_2] \qquad (17)$$

$$d[VI]/dt = 2k_{15}[V][O_2] \qquad (18)$$

Equations 13 and 17 have the same third-order form and correspond to rate-determining reduction of intermediate complex IXa by excess Va. According to the fit of the data in Figure S1[33] noted earlier and other considerations,[6b,32] this requires assembly of the appropriate activated complex. Equilibrium constant K_{15} in eq 17 must be less than 25 M^{-1} at 25 °C in nitrobenzene to account for the observed, simple orders in rate laws 13 and 14.[36,37]

Equations 14 and 18 have the same second-order form and correspond to rate-determining formation of respective intermediates IXb,c.[37] This is a reasonable conclusion because the copper(I) centers of V should be especially stabilized by X = Br and I.[31] Rate-determining formation of IXb,c precedes their very rapid reduction by excess Vb,c to give the ultimate products VIb,c, respectively, in ambient nitrobenzene.

Acknowledgment. This work was supported by Grants INT-8715384 and CHE-8717556 from the National Science Foundation, which are gratefully acknowledged. We thank Drs. Arthur Heiss and Ralph Weber of Bruker Instruments for help with the EPR measurements and Noralie Barnett and Amro El-Maradne for technical assistance.

Supplementary Material Available: Figure S1 (plot of $\Delta H_D^{\ddagger}$ vs $\Delta S_D^{\ddagger}$ for oxidation of excess copper(I) complexes $[LuCuX]_2$ (L is an *N,N,N',N'*-tetraalkyl diamine; X is Cl or Br) and Va by O_2 in nitrobenzene at ambient temperatures) (1 page). Ordering information is given on any current masthead page.

---

(34) The smallest and largest values of k_T at 25 °C with X = Br in rate law 10 are for the oxidations of $N_3Cu_3Ni(NS)Br_4$[7] and $N_3Cu_3Co(NS)_2Br_4$[10a] by O_2 in nitrobenzene, respectively.

(35) The data from refs 4, 7, and 10a can be used to construct a linear plot of $\Delta H_T^{\ddagger}$ vs $\Delta S_T^{\ddagger}$, which is one point of support for a common slow step in reactions 1, 3 and 9. Activation parameters $\Delta H_{14}^{\ddagger}$ and $\Delta S_{14}^{\ddagger}$ for second-order oxidation of Vb and Vc do not fit on this plot, which is further reason to favor the alternative oxidation mechanism in Scheme I.

(36) Significant concentrations of IXa-c would lead to denominators 1 + $K_{15}[V]$ in eqs 17 and 18, which would then not have the same forms as observed rate laws 13 and 14, respectively. An upper limit for $K_{15} = k_{15}/k_{-15}$ (Scheme I) is obtained by putting $K_{15}[V] < 0.1$ at the highest [V] employed (4.5 mM). Thus, $K_{15} < 25$ M^{-1} in nitrobenzene at 25 °C.

(37) Low-temperature kinetic data for *reversible*, second-order formation of the peroxocopper(II) complex $LCu_2O_2^{2+}$ (L is a binucleating amine ligand) in methylene chloride are as follows: $k_{15} = 533$ M^{-1} s^{-1} at -80 °C, with $\Delta H_{15}^{\ddagger} = 1.95$ kcal mol^{-1} and $\Delta S_{15}^{\ddagger} = -35$ cal deg^{-1} mol^{-1}.[38] The predicted equilibrium constant for formation of $LCu_2O_2^{2+}$ is 6 M^{-1} at 20 °C,[38] to be compared with our estimated upper limit $K_{15} < 25$ M^{-1} for formation of IXa-c in nitrobenzene at 25 °C. Predicted rate law 18 leads to the identification of k_{14} with $2k_{15}$. Similarity of $\Delta S_{15}^{\ddagger} = -(21 - 38)$ cal deg^{-1} mol^{-1} for oxidations of Vb, Vc (Table III), and LCu_2^{2+}[38] supports the mechanism in Scheme I and leads to the tentative identification of IXb and IXc as peroxocopper(II) complexes. Intermediates IXb and IXc appear to react very rapidly with Vb and Vc at ambient temperatures (see text). Reduction of peroxocopper species by copper(I) is less of a problem in particular low-temperature copper(I)/O_2 systems.[12,38]

(38) Cruse, R. W.; Kaderli, S.; Karlin, K. D.; Zuberbuhler, A. D. *J. Am. Chem. Soc.* **1988**, *110*, 6882 and references therein.